

# Regulating Competing Supramolecular Interactions Using Ligand Concentration

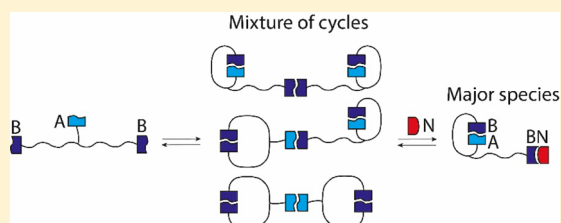
Abraham J. P. Teunissen,<sup>†,‡</sup> Tim F. E. Paffen,<sup>†,‡</sup> Gianfranco Ercolani,<sup>||</sup> Tom F. A. de Greef,<sup>\*,†,§</sup> and E. W. Meijer<sup>\*,†,‡</sup>

<sup>†</sup>Institute for Complex Molecular Systems, <sup>‡</sup>Laboratory of Macromolecular and Organic Chemistry, and <sup>§</sup>Computational Biology, Eindhoven University of Technology, P.O. Box 513, 5600 MB Eindhoven, The Netherlands

<sup>||</sup>Dipartimento di Scienze e Tecnologie Chimiche, Università di Roma Tor Vergata, Via della Ricerca Scientifica, 00133 Roma, Italy

**S** Supporting Information

**ABSTRACT:** The complexity of biomolecular systems inevitably leads to a degree of competition between the noncovalent interactions involved. However, the outcome of biological processes is generally very well-defined often due to the competition of these interactions. In contrast, specificity in synthetic supramolecular systems is usually based on the presence of a minimum set of alternative assembly pathways. While the latter might simplify the system, it prevents the selection of specific structures and thereby limits the adaptivity of the system. Therefore, artificial systems containing competing interactions are vital to stimulate the development of more adaptive and lifelike synthetic systems. Here, we present a detailed study on the self-assembly behavior of a  $C_{2v}$ -symmetrical tritopic molecule, functionalized with three self-complementary ureidopyrimidinone (UPy) motifs. Due to a shorter linker connecting one of these UPys, two types of cycles with different stabilities can be formed, which subsequently dimerize intermolecularly via the third UPy. The UPy complementary 2,7-diamido-1,8-naphthyridine (NaPy) motif was gradually added to this mixture in order to examine its effect on the cycle distribution. As a result of the  $C_{2v}$ -symmetry of the tritopic UPy, together with small differences in binding strength, the cycle ratio can be regulated by altering the concentration of NaPy. We show that this ratio can be increased to an extent where one type of cycle is formed almost exclusively.



## INTRODUCTION

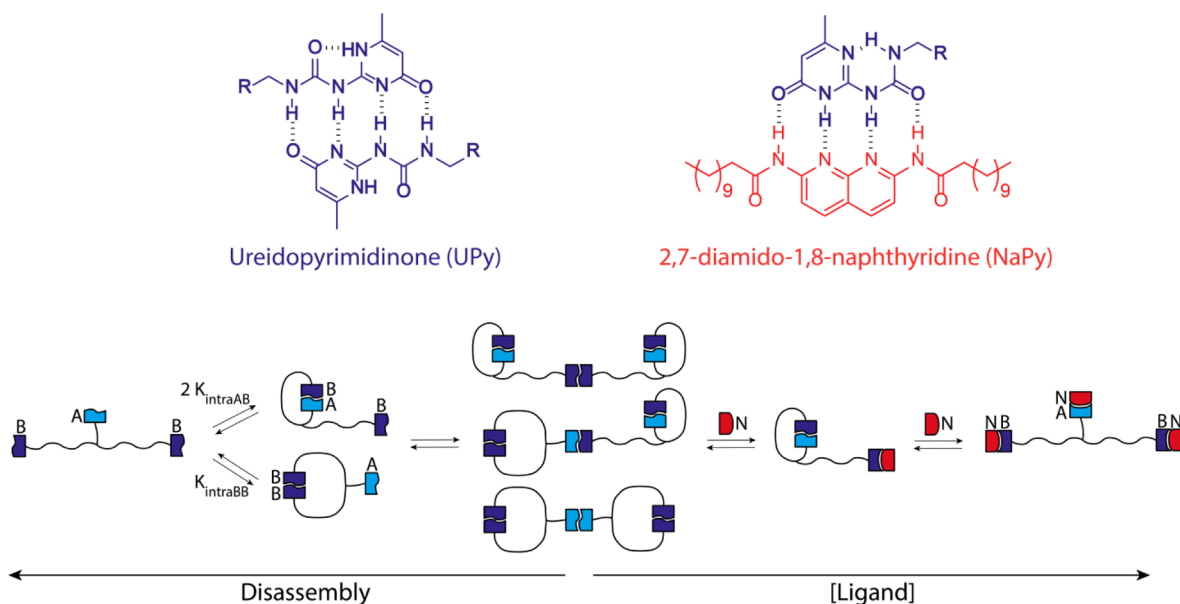
Competition plays a dominant role in all biological processes; it controls the evolution of species,<sup>1</sup> the growth of organs,<sup>2</sup> and even memory formation.<sup>3</sup> Especially on the molecular scale, the presence of competing pathways allows a delicate regulation of various processes, for example, the repair of double-strand DNA in eukaryotic cells depends on an interplay between two repair mechanisms<sup>4</sup> and RNA transcription in *E. coli* is regulated by the competition of seven different RNA polymerase  $\sigma$ -subunits.<sup>5</sup> While the presence of competition allows more flexibility in controlling the pathway desired, it also allows the possibility of undesired processes. Nature typically uses additives such as chaperones in protein folding<sup>6</sup> or competitive binders to regulate gene expression.<sup>7,8</sup> Multivalent scaffolds are another important way through which competing processes are controlled. Coupling multiple receptors together enhances their combined binding strength as a result of chelate cooperativity,<sup>9</sup> and this can have profound effects on the kinetics.<sup>10</sup> By regulating the number of mono- and multivalent receptors, equilibria can be influenced without the need of molecular changes in the binding motifs themselves, which is for example used by cells to probe ligand density.<sup>11</sup> Competing assembly pathways play an important role in nonlinear processes such as feedback-loops and regulatory networks.<sup>12</sup> As a result of their complex and often counterintuitive behavior,

a combined experimental and computational approach is often vital to gain an in-depth understanding, as shown by recent advances in systems biology.<sup>13,14</sup>

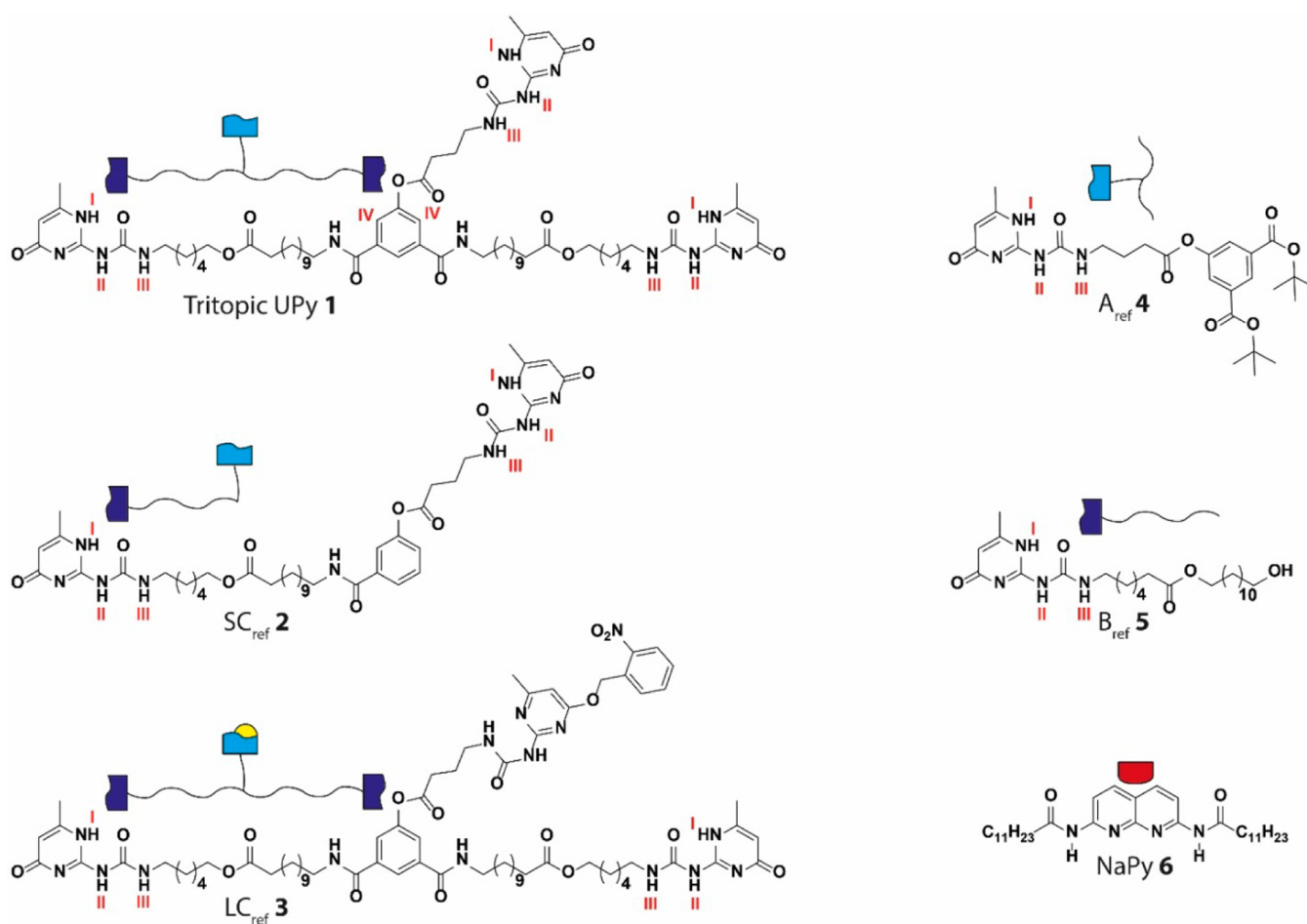
In recent years, multiple synthetic systems displaying semibiological behavior have been reported, such as logic gates,<sup>15,16</sup> self-sorting systems,<sup>17,18</sup> and the activation of a reaction by outcompeting a supramolecular protecting group.<sup>19</sup> While competing species are present in such systems, the large differences in binding strengths make them function in an on/off manner, without possessing the delicate regulation observed in biological systems. Other chemical systems have mimicked the multivalency found in biomolecules. In such systems, the binding motifs are generally not self-complementary<sup>20</sup> and positioned in a symmetrical manner, for example,  $C_3$ -symmetrical in trivalent pseudorotaxanes,<sup>21,22</sup>  $C_4$ -symmetrical on the 4 sides of a porphyrin,<sup>23,24</sup> or  $C_6$ -symmetrical in a hexavalent pyridine construct.<sup>25</sup> While these systems can form receptor–ligand contacts at different positions on the molecule, their symmetry makes the resulting species identical, preventing any competition. Additionally, the close proximity of the binding motifs often introduces a chelate cooperative effect,<sup>9,26,27</sup> limiting the amount of populated species.

Received: April 3, 2016

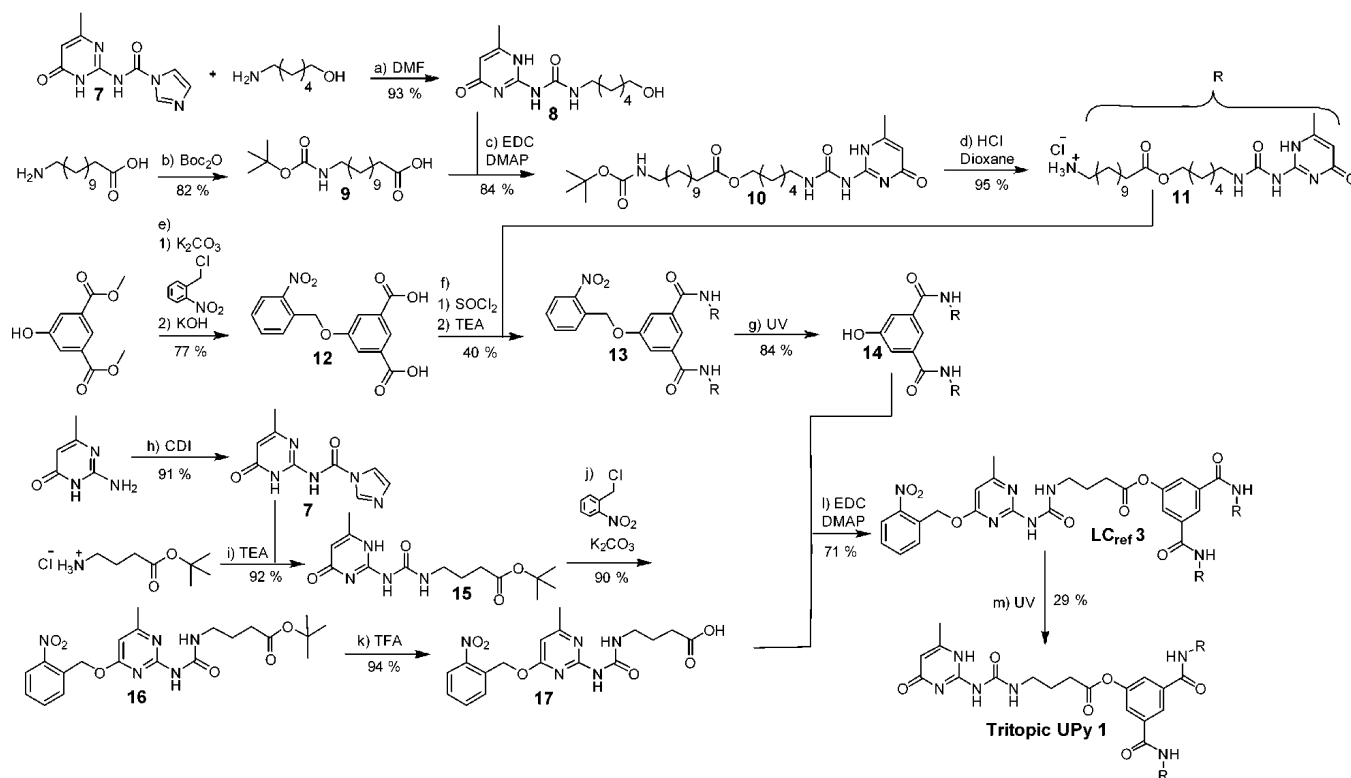
Published: May 10, 2016



**Figure 1.** Molecular structure of the UPy–UPy and UPy–NaPy dimers (top). Schematic representation of the cyclization and subsequent dimerization of a  $C_{2v}$ -symmetrical tritopic supramolecular building block, as well as its binding to a ligand (bottom). The tritopic UPy consists of one short linker connecting the UPy on the “A” position and two longer linkers connecting the UPys on position “B”. Due to this symmetry, two mutually exclusive type of cycles can be formed, which dimerize via the remaining third UPy. By varying the concentration of NaPy (N), the cycle distribution can be regulated, leading to a structure with all UPys bound to NaPy at higher ligand concentrations.



**Figure 2.** Molecular structures and schematic depiction of tritopic UPy 1 and reference compounds SC<sub>ref</sub> 2, LC<sub>ref</sub> 3, A<sub>ref</sub> 4, and B<sub>ref</sub> 5, as well as UPy complementary NaPy 6. Roman numerals are used to denote the specific protons referred to in the text.

Scheme 1. Synthesis of LC<sub>ref</sub> 3 and Tritopic UPy 1<sup>a</sup>

<sup>a</sup>Reagents and conditions: (a) DMF, room temperature, 16 h, 93%; (b) TEA, Boc<sub>2</sub>O, 60 °C, 16 h, 82%; (c) EDC, DMAP, room temperature, 60 °C, 16 h, 84%; (d) 3 M HCl in dioxane, room temperature, 16 h, 95%; (e) K<sub>2</sub>CO<sub>3</sub>, 1-(chloromethyl)-2-nitrobenzene, 85 °C, 2 h, KOH, H<sub>2</sub>O/THF, room temperature, 16 h, 77%; (f) SOCl<sub>2</sub>, DMF, room temperature, 4 h, TEA, room temperature, 16 h, 40%; (g) DCM, UV ( $\lambda = 315\text{--}400\text{ nm}$ ), room temperature, 10 h, 84%; (h) CDI, 80 °C, 16 h, 91%; (i) TEA, room temperature, 16 h, 92%; (j) K<sub>2</sub>CO<sub>3</sub>, 1-(chloromethyl)-2-nitrobenzene, 80 °C, 16 h, 90%; (k) TFA, room temperature, 16 h, 94%; (l) EDC, DMAP, room temperature, 16 h, 71%; (m) DCM, UV ( $\lambda = 315\text{--}400\text{ nm}$ ), room temperature, 5 h, 29%.

By delicately regulating competing processes via external stimuli, identical building blocks can be used for the synthesis of a variety of complexes,<sup>28,29</sup> in contrast to the more common approach of modifying binding constants by changing the molecular structure.<sup>30</sup> An elegant example is given by Otto et al., who have demonstrated that regulating the template concentration in a dynamic combinatorial library can lead to the amplification of specific receptors, and the strongest receptor is not necessarily amplified the most.<sup>31</sup> This shows that, similar as in natural systems, the introduction of competition can lead to complex behavior, but it does not necessarily lead to a lack of selectivity. For competition to be present, it is vital that different structures are formed as a result of a certain group that binds at different positions. Second, to act as a regulatory mechanism, the different structures formed in such a manner must be of comparable stability, potentially influenced by external stimuli.<sup>32</sup>

Our group has recently reported on a system where competing intra- and intermolecular interactions between supramolecular building blocks result in the buffering of catalytic activity over a broad concentration range.<sup>33</sup> This system is based on the self-complementary ureidopyrimidinone (UPy) motif and its binding to 2,7-diamido-1,8-naphthyridine (NaPy),<sup>34</sup> of which the latter can act as a phase-transfer catalyst in its unbound state.<sup>35</sup> It has been shown that the competition between linear and cyclic contacts formed by a ditopic UPy lead to a buffered concentration of NaPy chain-stopper, that is, the active catalyst. This work demonstrates that a combined

experimental and computation approach is also vital in synthetic systems to thoroughly understand competing processes.<sup>36</sup> To better mimic the way nature uses competition as a regulatory mechanism, we have now designed a system where the competition between structures of comparable stability is regulated via the binding of a small additional ligand.

We report the study of a C<sub>2v</sub>-symmetrical tritopic UPy (Figure 1). As a result of its symmetry, this compound can form two mutually exclusive types of cycles, which subsequently dimerize via the pendant third UPy, resulting in three different structures. Then the NaPy ligand is titrated to the mixture and its effect on the cycle distribution is examined. We show that, by altering the concentration or selectivity of NaPy, the ratio between the two types of cycles can be regulated. Using this approach, it is possible to exclusively form one type of cycle, without requiring changes to the molecular structure of the tritopic UPy.

## RESULTS AND DISCUSSION

**Design and Synthesis of Tritopic UPy 1 and Its Reference Compounds.** We have designed a C<sub>2v</sub>-symmetrical tritopic UPy molecule that is functionalized with one short linker connecting the UPy at position “A” (light blue, Figure 1) and two longer linkers of equal length connecting the UPy at the “B-positions” (dark blue, Figure 1). As a result of this architecture, it is possible to form two mutually exclusive type of cycles, that is, between an A and B-type UPys, or between both B-type UPys. The abundance of either cycle will depend

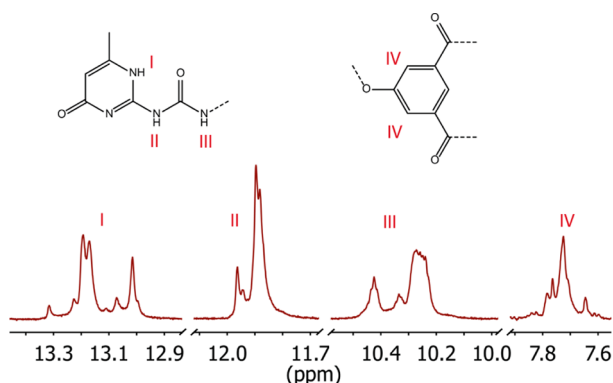


**Figure 3.** Partial  $^1\text{H}$  NMR spectrum of tritopic UPy **1** in  $\text{CDCl}_3$  at  $-15\text{ }^\circ\text{C}$  and 2 mM, showing multiple signals for protons I–IV due to the different conformations adopted by **1**. The UPy N–H signals originate from the combined A and B-type UPys in tritopic UPy **1**.

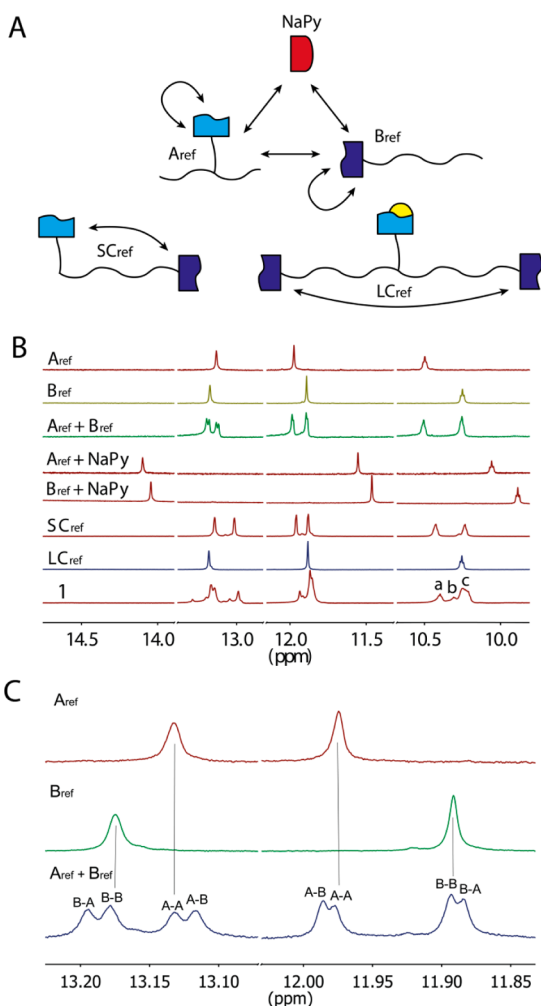


**Figure 4.** (A) Schematic overview of all UPy reference compounds and their interactions, as well as the NaPy ligand and its interactions with the A- and B-type UPys. (B) Partial  $^1\text{H}$  NMR spectra of proton I–III of all UPy reference compounds as well as compound **1** in  $\text{CDCl}_3$ ,  $T = -15\text{ }^\circ\text{C}$ ,  $c = 2\text{ mM}$  each. (C) Partial  $^1\text{H}$  NMR spectra of proton I and II of Aref **4** and Bref **5** in  $\text{CDCl}_3$ , showing that it is possible to distinguish between Aref–Aref, Aref–Bref, and Bref–Bref UPy dimers,  $T = -15\text{ }^\circ\text{C}$ ,  $c = 2\text{ mM}$  each.

on its relative stability, while the symmetric nature of the compound provides two ways of forming the A–B cycle,

making its formation entropically more favorable.<sup>37</sup> Additionally, a more indirect factor influencing the cycle distribution is predicted. Due to the high binding constant of the UPy motif ( $K_{\text{dim}} = 6 \times 10^7\text{ M}^{-1}$  in chloroform at  $25\text{ }^\circ\text{C}$ ),<sup>38</sup> unbound UPys are generally unfavorable, therefore the cyclic structures will dimerize via the pendent binding position. Depending on the type of dimerized cycle that is formed, three different types of linear dimers are created (i.e., A–A, A–B, and B–B). The different molecular connectivity of the A and B-type UPys results in small differences in the stability of these dimers (vide infra), which influences the cycle distribution as well; for example, a relatively high stability of the A–A dimers favors the formation of B–B cycles. Similarly, association of a NaPy (N) that can bind to the UPy motif will be governed by the stabilities of the A–N and B–N dimers. Additionally, ligand binding is governed by statistical factors; that is, there are twice as many B as A groups, making it more likely to form B–N contacts. Such ligand binding competes with intramolecular cycle formation, giving rise to a complex interplay of interactions.

As mentioned, to alter the stability of both type of cycles, the linker connecting the A-type UPy is slightly shorter than that connecting the B-type UPys. In addition to this, we synthesized the A-type UPy in close proximity to an ester moiety, with the goal to change its chemical shift compared to the B-type UPys and thereby simplify characterization by  $^1\text{H}$  NMR (Figure 2). To further aid characterization of the different configurations adopted by **1**, reference compounds SCref **2**, LCref **3**, Aref **4**, and Bref **5** were synthesized as well. While SCref **2** acts as a model for the smaller A–B cycle, LCref **3** has a UPy group on the A position covalently protected by an UV-labile o-nitrobenzyl group and therefore acts as a reference compound for the larger B–B cycle. The linear, intermolecular, interactions between the A and B-type UPys potentially formed by **1** are represented by Aref **4** and Bref **5**, respectively. In addition to these reference compounds, UPy complementary NaPy **6** is used in this study. Finally, NaPy is unable to form stable homodimers in  $\text{CDCl}_3$ .

Tritopic UPy **1** was synthesized via the same route as LCref **3**, starting from the formation of UPy alcohol **8** (Scheme 1). UPy **8** was then coupled to Boc-protected amino acid **9** via EDC mediated esterification, resulting in UPy **10**. Subsequent deprotection using HCl resulted in UPy amine **11**. The alcohol moiety of commercially available dimethyl 5-hydroxyisophthalate was protected using 1-(chloromethyl)-2-nitrobenzene and the methylester was hydrolyzed using aqueous KOH, resulting in **12**. Compound **12** was subsequently converted in the diacyl chloride using  $\text{SOCl}_2$  and coupled to **11**, resulting in ditopic UPy **13** which was deprotected using UV-light, resulting in phenol **14** containing both B-type UPys. To introduce the UPy on the A position, CDI activated isocytosine **7** was coupled to commercially available 4-(tert-butoxy)-4-oxobutan-1-aminium chloride resulting in UPy **15**. This UPy **15** was then protected using 1-(chloromethyl)-2-nitrobenzene yielding **16**, which was deprotected by TFA to give UPy **17**. Ester formation between **14** and **17** resulted in LCref **3**, which upon UV-irradiation gave tritopic UPy **1**. Further details, as well as the synthesis and characterization of SCref **2**, Aref **4**, Bref **5**, and NaPy **6** can be found in the Supporting Information.

**$^1\text{H}$  NMR Analysis of Tritopic UPy **1** and Its Reference Compounds.** A solution of tritopic UPy **1** was analyzed by  $^1\text{H}$  NMR ( $c = 2\text{ mM}$ ,  $\text{CDCl}_3$ ), and the sample was cooled to  $-15\text{ }^\circ\text{C}$  to improve signal analysis. Multiple signals were observed for all UPy N–H protons, as well as the protons of the aromatic

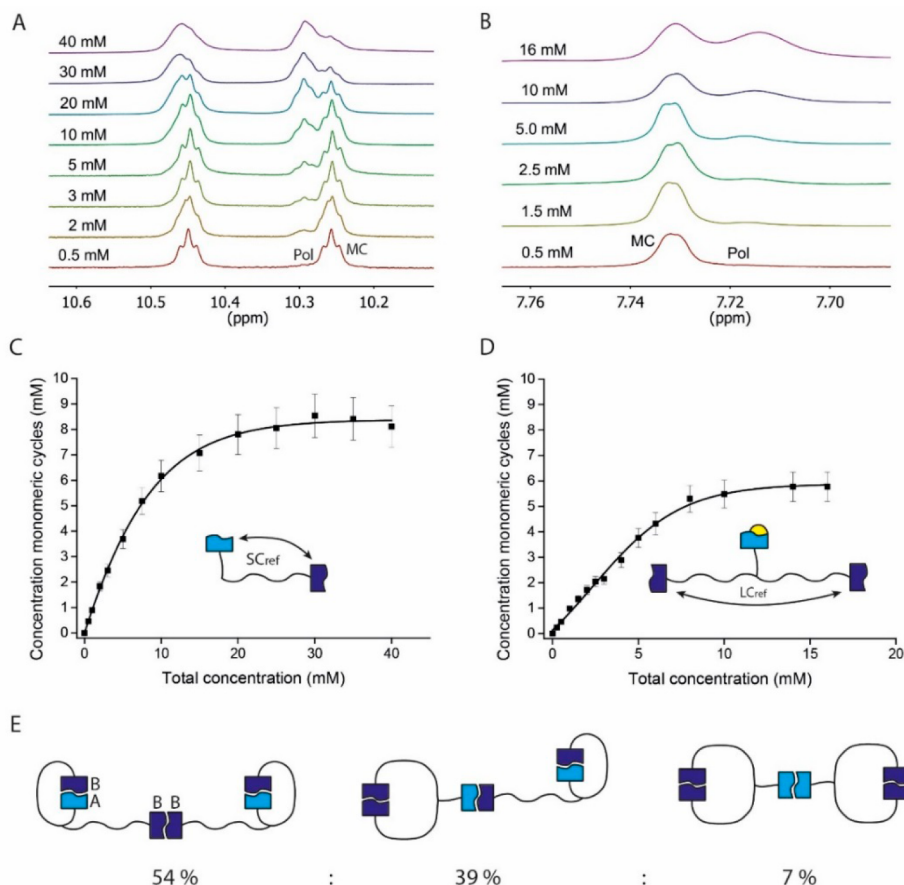


**Figure 5.** (A,B) Partial  $^1\text{H}$  NMR spectra of proton III of the B-type UPy in  $\text{SC}_{\text{ref}} 2$  and proton IV in  $\text{LC}_{\text{ref}} 3$  at various concentrations in  $\text{CDCl}_3$  at  $-15^\circ\text{C}$ . Signals associated with monomeric cycles are annotated with MC, signals associated with higher order cycles and polymers with Pol. This signal assignment was based on the expected concentration dependent behavior of ditopic molecules.<sup>41</sup> (C,D) Concentration of monomeric cycles versus the total concentration. The plateau concentration that is reached is equal to the effective molarity ( $\text{EM} = K_{\text{intra}}/K_{\text{inter}}$ ) of the monomeric cycles (8.2 mM for  $\text{SC}_{\text{ref}} 2$  and 5.8 mM for  $\text{LC}_{\text{ref}} 3$ ). The fraction of monomeric cycles was calculated by dividing the area of the peak assigned to MC by the total peak area corresponding to the specific proton. Considering the errors on weighing (1%),<sup>42</sup> pipetting (1%)<sup>43</sup> and NMR integration/deconvolution (5%),<sup>44</sup> we used standard error propagation techniques to determine the standard deviation to be  $\approx 5\%$ . The errors bars depicted two times the standard deviation, i.e., 10%. The solid line is used to guide the eye. (E) Expected speciation of tritopic UPy 1 at 2 mM in  $\text{CDCl}_3$  based on the EMs of  $\text{SC}_{\text{ref}} 2$  and  $\text{LC}_{\text{ref}} 3$ . Assuming equal binding constants of UPy dimerization, the expected fraction of A-B cycles was calculated as  $2\text{EM}_{\text{AB}} / (2\text{EM}_{\text{AB}} + \text{EM}_{\text{BB}})$  and the fraction of B-B cycles as  $\text{EM}_{\text{BB}} / (2\text{EM}_{\text{AB}} + \text{EM}_{\text{BB}})$ . The distribution of dimeric cycles was calculated as follows: fraction of dimeric A-B cycles = (fraction A-B cycles)<sup>2</sup>, fraction of dimer consisting of an A-B cycle connected to a B-B cycle =  $2 \times (\text{fraction A-B cycles})(\text{fraction B-B cycles})$ , fraction of dimeric B-B cycles = (fraction B-B cycles)<sup>2</sup>.

core, suggesting that **1** forms a complex mixture of species in solution (Figure 3). No changes were observed over the course of 3 h, suggesting thermodynamic equilibrium was reached fast, which could be expected considering the short lifetime of the UPy-UPy interaction in  $\text{CDCl}_3$  (0.12 s at  $25^\circ\text{C}$ ).<sup>38</sup> Small changes in the concentration ( $c = 1\text{--}7\text{ mM}$ ) did not lead to any significant changes in the  $^1\text{H}$  NMR spectrum (See Figure S7 for  $^1\text{H}$  NMR spectra).

In order to interpret the  $^1\text{H}$  NMR of **1** correctly, we chose to compare its  $^1\text{H}$  NMR spectrum to that of the reference compounds taken under identical conditions, that is,  $c = 2\text{ mM}$  at  $-15^\circ\text{C}$  in  $\text{CDCl}_3$  (Figure 4). Study of the  $^1\text{H}$  NMR spectra of the reference compounds revealed that all UPy-UPy and UPy-NaPy interactions can be identified using a unique chemical shift (Figures 4B and S1). Interestingly, using the respective protons I and II in  $\text{A}_{\text{ref}} 4$  and  $\text{B}_{\text{ref}} 5$ , it even proved possible to discriminate between linear A-A, A-B, and B-B UPy contacts (Figure 4C). Deconvolution of these signals showed that in an equimolar mixture,  $\text{A}_{\text{ref}}\text{-A}_{\text{ref}}$  and  $\text{B}_{\text{ref}}\text{-B}_{\text{ref}}$  dimers are more abundant than  $\text{A}_{\text{ref}}\text{-B}_{\text{ref}}$  dimers (see Figure S3

for more details). This suggests that the different connectivity of the A- and B-type UPys has led to different stabilities of the various types of contacts. Likely, the close proximity of the A-type UPys to an ester moiety and aromatic core has led to a reduced binding strength, as has been shown for UPys with other types of polar side-chains.<sup>39,40</sup>

Since tritopic UPy **1** has a similar molecular architecture as its reference compounds, it is expected that identical interactions will lead to similar chemical shifts, thereby providing means to determine the speciation of tritopic UPy **1**. In addition to this, quantitative knowledge about the stability of the cycles formed by **1** is vital for obtaining a complete understanding of its behavior.

Using  $\text{SC}_{\text{ref}} 2$  and  $\text{LC}_{\text{ref}} 3$ , the effective molarities (denoting the stability of the cycles and defined as  $\text{EM} = K_{\text{intra}}/K_{\text{inter}}$ ) of the monomeric A-B and B-B cycle were determined to be 8.3 and 5.8 mM, respectively. This was indicated by the maximal attainable concentration of these species in  $\text{CDCl}_3$  (Figure 5).<sup>41</sup> These effective molarities, together with the symmetry factor of 2 for the formation of the A-B cycle, results in an expected

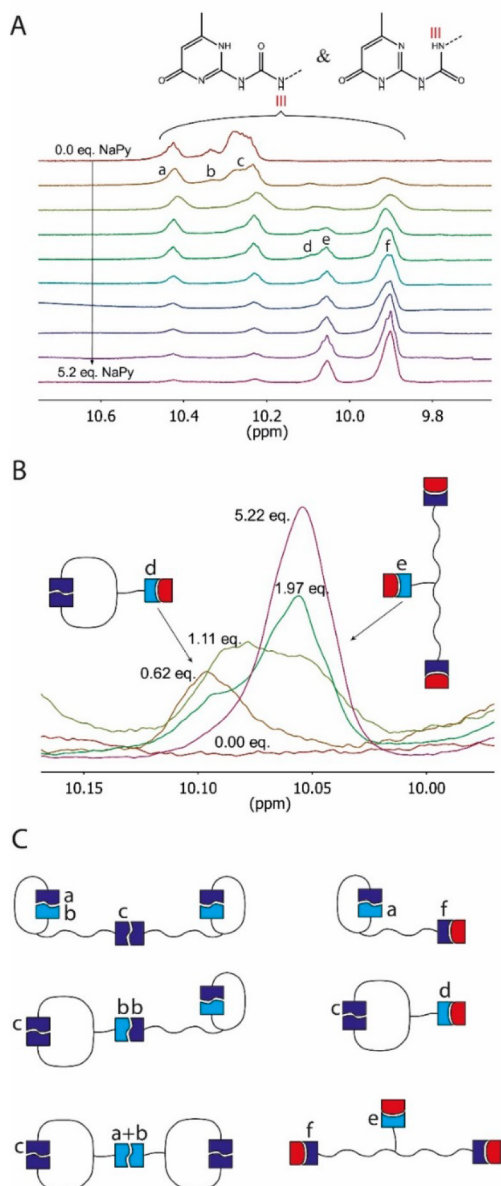


**Figure 6.** (A) Partial  $^1\text{H}$  NMR spectrum of UPy proton III in **1** with various amounts of NaPy **6** in  $\text{CDCl}_3$  at  $-15^\circ\text{C}$  and  $c = 2\text{ mM}$ . (B) Zoom-in of Figure 6A, depicting the shape of signals d and e as a function of the equivalents of NaPy **6** added. (C) Schematic depiction of the species present in solution showing the specific interactions assigned to the various  $^1\text{H}$  NMR signals.

74% of A–B cycles and 26% B–B cycles for compound **1** at 2 mM. Assuming that the linear contacts connecting these cycles are of equal stability, dimerization of the cycles will result in the statistical distribution depicted in Figure 5E. In conclusion, by studying the reference compounds we obtained an estimate of the speciation of **1**, as well as the means of interpreting its  $^1\text{H}$  NMR spectrum. This allows us to study the titration of tritopic UPy **1** with NaPy **6** and to record the changes in composition of the afforded species of **1** when **6** is added.

**Determining the Speciation of Tritopic UPy **1** in the Presence of Different Amounts of NaPy **6**.** The UPy-complementary supramolecular unit 2,7-diamido-1,8-naphthyrindine (NaPy) **6** was titrated to tritopic UPy **1** in order to study its influence on the cycle distribution of **1**. Since UPy proton III gave the best signal separation it was used to determine the

exact speciation of tritopic UPy **1**. During this titration 6 different signals could be distinguished (Figure 6A). By comparison with the reference compounds, signals a and c could be assigned to the A- and B-type UPys in the monomeric A–B cycle. Signal c also contained the linear and/or cyclic B–B interactions, while these could be distinguished in LC<sub>ref</sub> **3**, signal overlap prevented this for tritopic UPy **1**. In a similar fashion, signals d and e were assigned to A–N heterodimers.

As shown in Figure 6B, the addition of NaPy first leads to the appearance of signal d, which is converted into signal e upon further addition of NaPy. This behavior strongly suggests that signal d originates from an A–N contact connected to a B–B cycle, while signal e originates from an A–N contact in a tritopic UPy with all UPys bound to NaPy. Signal f most likely originates from a B–N contact. As a result, the five most abundant signals that are observed during the NaPy titration can be identified using the reference compounds, with only signal b lacking. After considering several explanations for signal b, we have concluded that it most likely originates from linear A–B and small amounts of linear A–A interactions (see the Supporting Information for further details). By comparing the  $^1\text{H}$  NMR spectra of the reference compounds with that of tritopic UPy **1**, we have obtained a likely assignment of the signals observed during the titration of NaPy to **1** (Figure 6C). Since some of these signals are attributed to multiple types of contacts, it is difficult to infer the species distribution directly from the data. To overcome this difficulty and validate our assignment, we have constructed a thermodynamic binding model and subsequently fitted it to the titration data.

**Modeling the Speciation of Tritopic UPy **1** as a Function of NaPy Concentration.** The thermodynamic binding model used to fit the NaPy titration data includes all possible monomeric and dimeric species of tritopic UPy **1**, cyclized and NaPy bound species (for details, see the Supporting Information). The model input parameters are binding constants for A–A-, A–B-, and B–B-type UPy contacts ( $K_{AA}$ ,  $K_{AB}$ , and  $K_{BB}$ , respectively), binding constants for both types of UPy–NaPy contacts ( $K_{AN}$  and  $K_{BN}$ ), and the effective molarities of both small A–B and large B–B monomeric cycles ( $EM_{SC}$  and  $EM_{LC}$ , respectively). Parameter bounds were applied to avoid the outcome of unrealistic parameter values. Given the simple aliphatic chain connecting the B-type UPys, we assumed the binding constant of linear B–B and B–N contacts to be similar to literature values ( $6 \times 10^7\text{ M}^{-1}$  and  $5 \times 10^6\text{ M}^{-1}$ , respectively)<sup>38,34</sup> and allowed a relatively small deviation of 5%. Since it is unlikely that the other type of UPy and NaPy contacts are significantly stronger, an upper limit of  $10^8\text{ M}^{-1}$  was introduced for these contacts. Furthermore,  $K_{AA}$  and  $K_{AB}$  were given lower limits of  $10^5\text{ M}^{-1}$  and  $K_{AN}$  a lower limit of  $10^3\text{ M}^{-1}$  (in line with reference experiments, see the Supporting Information for further details). Lastly, the effective molarities were constrained to the values that were obtained from the ditopic reference compounds SC<sub>ref</sub> **2** and LC<sub>ref</sub> **3**, allowing for a 10% deviation due to potential experimental error.

A large number of nonlinear least-squares optimizations with different initial values were performed to ensure that the global minimum was obtained (Figure 7A). Since the model parameters are highly correlated, this results in a collection of parameter values that give equally good fits (Figure 7B). Nonetheless, using this collection of optimized parameter values to calculate the molecular speciation plots resulted in almost identical species distributions (Figure 7C and D). Thus,

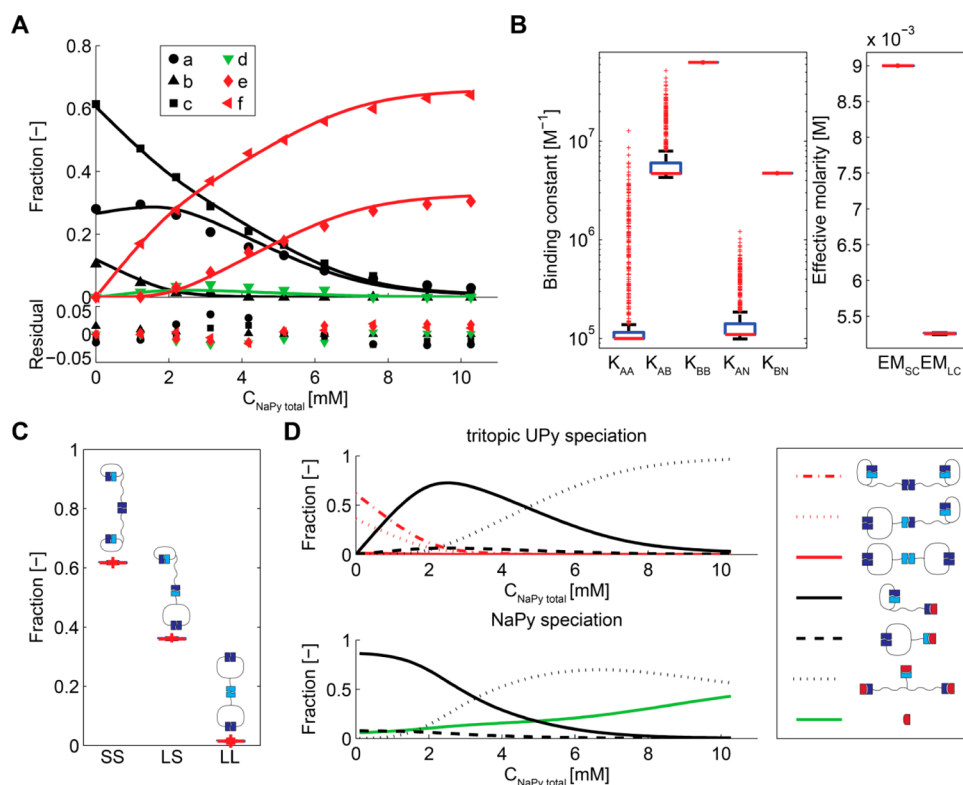


**Figure 7.** (A) Normalized peak intensities of  $^1\text{H}$  NMR spectra of signals observed for proton III during titration of NaPy **6** to tritopic UPy **1** (symbols) and the best fit based on the thermodynamic model (lines). (B) Fit parameter values of all nonlinear least-squares optimizations that have a squared 2-norm residual within 5% of the optimal parameter set. (C) Calculated distribution of cyclized tritopic UPy dimers based on the parameter values of the best fits. (D) Average of the calculated speciation during NaPy titration, based on the parameter values of the best fits. Note that the 95% confidence interval is smaller than the line width of the plot, thus it was omitted.

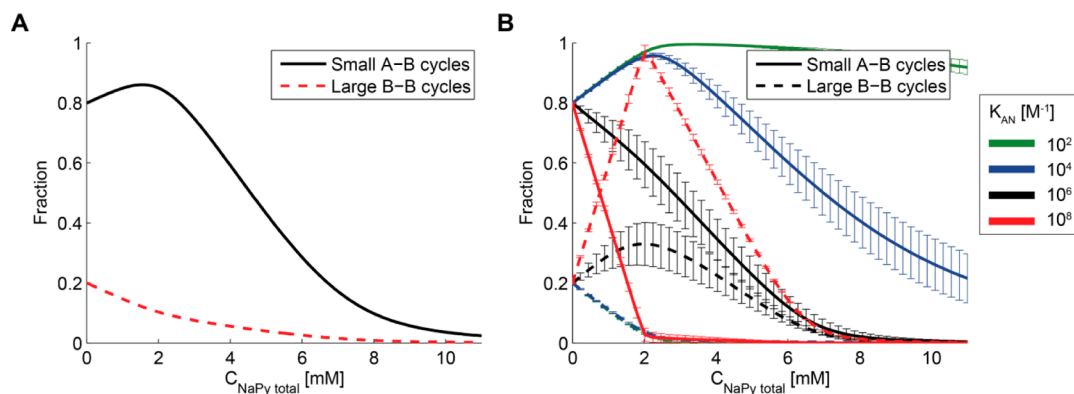


**Figure 8.** (A) Calculated fractions of small and large cycles during NaPy titration, based on the model parameters of the best fits. The 95% confidence interval is smaller than the line width of the plot, and thus, it was omitted. (B) Average simulated fractions of small and large cycles during NaPy titration using various values of  $K_{\text{AN}}$  and the model parameters of the best fits. The exact values of  $K_{\text{AN}}$  are shown next to the color bar. The error bars denote the 95% confidence interval, calculated as two times the standard deviation.

while the parameter values cannot be determined exactly, the species distribution can. The measured speciation of tritopic UPy **1** in the absence of NaPy **6** is quite similar to the one predicted, assuming equal binding strengths (Figures 5E and 7C). However, as a result of the differences in UPy–UPy binding strengths, that is,  $B-B > A-B > A-A$ , the fraction of dimerized A–B cycles is slightly higher than expected, at the expense of the B–B cycles. Upon the addition of NaPy **6**, the relatively weak linear UPy–UPy contacts connecting the dimerized cycles are disrupted first, resulting in monomeric cycles with the third UPy bound to NaPy. At higher equivalents

of NaPy, the cycles open up, resulting in a tritopic UPy with NaPy bound to all UPys.

Interestingly, signal “a” first increases and subsequently decreases during the NaPy titration, implying that the fraction of small A–B cycles is increased upon addition of small amounts of NaPy. Using the fitted species distribution, the fractions of small and large cycles during the titration were calculated, confirming this observation (Figure 8A). The fraction of small cycles increases from 0.80 to 0.86, which is attributed to  $K_{\text{BN}}$  being approximately 1 order of magnitude higher than  $K_{\text{AN}}$ , along with the fact that there are two B-type

UPys to every A-type UPy. Both of these effects increase the likelihood of NaPy binding to a B-type UPy, which subsequently stabilizes the small A–B cycle with respect to the larger B–B cycle. Thus, at low equivalents, NaPy 6 acts as a promoter for the formation of the small A–B cycle in tritopic UPy 1.

Having demonstrated the amplifying effect of NaPy 6 on the cycle ratio, we investigated the extent to which NaPy can influence the cycle distribution. Interestingly, decreasing the value of  $K_{AN}$  in the simulation even further allows the exclusive formation of small A–B cycles, while increasing  $K_{AN}$  allows the exclusive formation of large B–B cycles (Figure 8B). In this manner, the concentration and selectivity of NaPy can be used to regulate the fraction of each type of cycle, without altering the molecular structure of tritopic UPy 1.

## CONCLUSIONS

We report on the self-assembly behavior of a  $C_{2v}$ -symmetrical tritopic UPy building block, with special emphasis on the competition between two modes of intramolecular cycle formation and how this equilibrium is influenced by ligand binding. We have shown that with the correct reference compounds and molecular design it is possible to quantify the complex intra- and intermolecular interactions formed by this molecule. The resulting speciation stems from differences in cycle stability, symmetry factors, and small differences in binding strength, as corroborated by detailed computational modeling. By varying the concentration and selectivity of the ligand, the fraction of each type of intramolecular cycle can be precisely controlled. We show that using this approach it is possible to exclusively form either type of cycle, without changing the molecular structure of the tritopic UPy. Our study also highlights the difficulties associated with characterizing multitopic systems at the molecular level and shows that even a relatively simple multitopic building block requires a combined experimental and computational approach. We foresee that the work presented in this paper is an important contribution to the further understanding and development of multivalent systems with unexpected emerging properties.

## ASSOCIATED CONTENT

### Supporting Information

The Supporting Information is available free of charge on the ACS Publications website at DOI: 10.1021/jacs.6b03421.

Detailed experimental procedures, complete characterization of compounds and supramolecular interactions, as well as further information on the computational model (PDF)

## AUTHOR INFORMATION

### Corresponding Authors

\*e.w.meijer@tue.nl

\*t.f.a.d.greef@tue.nl

### Notes

The authors declare no competing financial interest.

## ACKNOWLEDGMENTS

We like to thank Dr. Anja Palmans for useful discussions about synthesis. This work is financed by the Dutch Organization for Scientific Research (NWOTOP and ECHO-STIP, Grant Nos. 10007851 and 717.013.001), the Dutch Ministry of Education, Culture and Science (Gravity program 024.001.035), and the

European Research Council (FP7/2007-2013 and H2020/2014-2020, ERC Advanced Grant No. 246829 and ERC Starting Grant No. 677313).

## REFERENCES

- (1) Wilson, A. J. *Heredity* **2014**, *112*, 70.
- (2) De La Cova, C.; Abril, M.; Bellosta, P.; Gallant, P.; Johnston, L. a. *Cell* **2004**, *117*, 107.
- (3) Han, J.; Kushner, S. A.; Yiu, A. P.; Cole, C. J.; Matynia, A.; Brown, R. a.; Neve, R. L.; Guzowski, J. F.; Silva, A. J.; Josselyn, S. A. *Science* **2007**, *316*, 457.
- (4) Kass, E. M.; Jasin, M. *FEBS Lett.* **2010**, *584*, 3703.
- (5) Maeda, H.; Fujita, N.; Ishihama, A. *Nucleic Acids Res.* **2000**, *28*, 3497.
- (6) Hartl, F. U.; Hayer-Hartl, M. *Science* **2002**, *295*, 1852.
- (7) Jens, M.; Rajewsky, N. *Nat. Rev. Genet.* **2014**, *16*, 113.
- (8) Fabian, M. R.; Sonenberg, N.; Filipowicz, W. *Annu. Rev. Biochem.* **2010**, *79*, 351.
- (9) Ercolani, G.; Schiaffino, L. *Angew. Chem., Int. Ed.* **2011**, *50*, 1762.
- (10) Badjić, J. D.; Cantrill, S. J.; Stoddart, J. F. *J. Am. Chem. Soc.* **2004**, *126*, 2288.
- (11) Meyer, A. S.; Zweemer, A. J. M.; Lauffenburger, D. A. *Cell Syst.* **2015**, *1*, 25.
- (12) Genot, A. J.; Fujii, T.; Rondelez, Y. *Phys. Rev. Lett.* **2012**, *109*, 208102.
- (13) Kitano, H. *Nature* **2002**, *420*, 206–210.
- (14) Todd, E. M.; Zimmerman, S. C. *J. Chem. Educ.* **2009**, *86*, 638.
- (15) Pischel, U.; Uzunova, V. D.; Remón, P.; Nau, W. M. *Chem. Commun.* **2010**, *46*, 2635.
- (16) Komatsu, H.; Matsumoto, S.; Tamaru, S. I.; Kaneko, K.; Ikeda, M.; Hamachi, I. *J. Am. Chem. Soc.* **2009**, *131*, 5580.
- (17) Wu, A.; Isaacs, L. *J. Am. Chem. Soc.* **2003**, *125*, 4831.
- (18) Safont-Sempere, M. M.; Fernández, G.; Würthner, F. *Chem. Rev.* **2011**, *111*, 5784.
- (19) Smulders, M. M. J.; Nitschke, J. R. *Chem. Sci.* **2012**, *3*, 785.
- (20) Hoogenboom, R.; Fournier, D.; Schubert, U. S. *Chem. Commun.* **2008**, 155.
- (21) Balzani, V.; Clemente-León, M.; Credi, A.; Lowe, J. N.; Badjić, J. D.; Stoddart, J. F.; Williams, D. J. *Chem. - Eur. J.* **2003**, *9*, 5348.
- (22) Nowosinski, K.; von Krbek, L. K. S.; Traulsen, N. L.; Schalley, C. A. *Org. Lett.* **2015**, *17*, 5076.
- (23) Sun, H.; Guo, K.; Gan, H.; Li, X.; Hunter, C. A. *Org. Biomol. Chem.* **2015**, *13*, 8053.
- (24) Hunter, C. A.; Misuraca, M. C.; Turega, S. M. *J. Am. Chem. Soc.* **2011**, *133*, 20416.
- (25) Hogben, H. J.; Sprafke, J. K.; Hoffmann, M.; Pawlicki, M.; Anderson, H. L. *J. Am. Chem. Soc.* **2011**, *133*, 20962.
- (26) Montoro-García, C.; Camacho-García, J.; López-Pérez, A. M.; Mayoral, M. J.; Bilbao, N.; González-Rodríguez, D. *Angew. Chem., Int. Ed.* **2016**, *55*, 223.
- (27) Fonseca Guerra, C.; Zijlstra, H.; Paragi, G.; Bickelhaupt, F. M. *Chem. - Eur. J.* **2011**, *17*, 12612.
- (28) McQuirk, C. M.; Stern, C. L.; Mirkin, C. A. *J. Am. Chem. Soc.* **2014**, *136*, 4689.
- (29) Song, Y.; Cheng, P.; Zhu, L.; Moore, E. G.; Moore, J. S. *J. Am. Chem. Soc.* **2014**, *136*, 5233.
- (30) Ogi, S.; Fukui, T.; Jue, M. L.; Takeuchi, M.; Sugiyasu, K. *Angew. Chem., Int. Ed.* **2014**, *53*, 14363.
- (31) Corbett, P. T.; Sanders, J. K. M.; Otto, S. *J. Am. Chem. Soc.* **2005**, *127*, 9390.
- (32) Grzybowski, B. A.; Wilmer, C. E.; Kim, J.; Browne, K. P.; Bishop, K. J. M. *Soft Matter* **2009**, *5*, 1110.
- (33) Rodríguez-Llansola, F.; Meijer, E. W. *J. Am. Chem. Soc.* **2013**, *135*, 6549.
- (34) Wang, X. Z.; Li, X. Q.; Shao, X.-B.; Zhao, X.; Deng, P.; Jiang, X. K.; Li, Z. T.; Chen, Y. Q. *Chem. - Eur. J.* **2003**, *9*, 2904.
- (35) Teunissen, A. J. P.; van der Haas, R. J. C.; Vekemans, J. A. J. M.; Palmans, A. R. A.; Meijer, E. W. *Bull. Chem. Soc. Jpn.* **2016**, *89*, 308.



- (36) Paffen, T. F. E.; Ercolani, G.; de Greef, T. F. A.; Meijer, E. W. J. *Am. Chem. Soc.* **2015**, *137*, 1501.
- (37) Ercolani, G.; Piguet, C.; Borkovec, M.; Hamacek, J. *J. Phys. Chem. B* **2007**, *111*, 12195.
- (38) Söntjens, S. H. M.; Sijbesma, R. P.; van Genderen, M. H. P.; Meijer, E. W. J. *Am. Chem. Soc.* **2000**, *122*, 7487.
- (39) De Greef, T. F. A.; Nieuwenhuizen, M. M. L.; Sijbesma, R. P.; Meijer, E. W. J. *Org. Chem.* **2010**, *75*, 598.
- (40) De Greef, T. F. A.; Kade, M. J.; Feldman, K. E.; Kramer, E. J.; Hawker, C. J.; Meijer, E. W. J. *Polym. Sci., Part A: Polym. Chem.* **2011**, *49*, 4253.
- (41) Ercolani, G.; Mandolini, L.; Mencarelli, P.; Roelens, S. J. *Am. Chem. Soc.* **1993**, *115*, 3901.
- (42) [www.mt.com](http://www.mt.com).
- (43) <http://www.hamiltoncompany.com/products/syringes-and-needles>.
- (44) Bain, A. D.; Fahie, B. J.; Kozluk, T.; Leigh, W. J. *Can. J. Chem.* **1991**, *69*, 1189.